Article

Discovery Medicine 2023; 35(179): 1134–1146
https://doi.org/10.24976/Discov.Med.202335179.110

Eriocitrin Alleviates Inflammation and Oxidative Stress in Subarachnoid Hemorrhage by Regulating DUSP14

Liuqing Sheng[1,2], Xiaolong Yao[2], Jianfeng Ye[2], Zhizhong Wang[2], Yinchun Chen[2], Jun Li[2], Mingchang Li[1,*]

[1]Department of Neurosurgery, Renmin Hospital of Wuhan University, 430060 Wuhan, Hubei, China
[2]Department of Neurosurgery, The Third People's Hospital of Hubei Province, 430014 Wuhan, Hubei, China
*Correspondence: limingchang197101@163.com (Mingchang Li)
Published: 1 December 2023

Background: Inflammation and oxidative stress (OS) are major causes of aneurysmal subarachnoid hemorrhage (aSAH)-induced early brain injury (EBI). Eriocitrin (EC), a flavonoid compound, has anti-inflammatory and antioxidant actions. However, there is still no relevant studies on the role of EC in SAH. Accordingly, this research aims to clarify the anti-OS and anti-inflammatory efficacy of EC in SAH.

Method: Rat SAH model was established *in vivo* and administered with Eriocitrin (25 mg/kg). *In vitro*, BV2 cells were exposed to oxyhemoglobin (OxyHb) for 24 hours and pretreated with Eriocitrin (1 uM/mL, 2 uM/mL, 4 uM/mL) for 30 minutes. Water maze experiments and neurological function scores were conducted to assess cognitive and motor function. TdT-mediated dUTP Nick-End Labeling (TUNEL) staining was used to detect cortical cell apoptosis. Enzyme-linked immunosorbent assay (ELISA) and polymerase chain reaction (PCR) were used to detect the inflammatory factors and malondialdehyde (MDA), as well as the expression of superoxide dismutase (SOD) and glutathione peroxidase (GSH-px). Western blots were used to semi quantify nuclear factor erythroid-2-related factor 2 (Nrf2), nuclear factor-κB (NF-κB), dual specificity phosphatase 14 (DUSP14) expression.

Results: The findings suggest that EC (25 mg/kg) reduced SAH-induced central nervous system (CNS) damage, neuronal apoptosis, inflammatory reactions and OS. Regarding a mechanistic study, EC enhanced Nrf2 and NF-κB by increasing DUSP14 activation, thereby reducing the inflammatory cytokines interleukin (IL)-1β, tumor necrosis factor (TNF)-α, and IL-6. In addition, EC decreased MDA while markedly elevating SOD and enhancing GSH-px. Furthermore, specifically inhibiting DUSP14 expression via using protein-tyrosine-phosphatase (PTP) inhibitor IV, neutralized the protective action of EC and aggravated inflammation and OS. *In vitro* experiments of OxyHb-induced BV2 cells revealed that EC promoted Nrf2 while markedly suppressing NF-κB by increasing DUSP14 activation, thereby reducing the concentrations of the above inflammatory cytokines. Moreover, EC decreased MDA while evidently increasing SOD and GSH-px.

Conclusion: In summary, this paper lays a theoretical grounding for EC treatment of SAH-induced inflammatory reactions and OS by regulating DUSP14.

Keywords: SAH; eriodocitrin; DUSP14; NF-κB; inflammatory; oxidative stress

Introduction

Aneurysmal subarachnoid hemorrhage (aSAH), a severe neurosurgical disease, presents high mortality and disability. Its annual prevalence is 10.5/100,000 population, second only to ischemic stroke and hypertensive cerebral hemorrhage, ranking third in cerebrovascular disease. At present, studies have found that the pathophysiological mechanism of aSAH is complex [1,2]. Post-SAH cerebral vasospasm (CVS) and early brain injury (EBI) are prime reasons for disability and death [3]. An increasing number of experts have increasingly recognized the essential role of EBI [4]. EBI refers to a series of pathophysiological brain damage events within 72 hours after SAH. Its pathogenic mechanism is complex and diverse, may be the result of the joint action of many factors and multiple pathways, especially neuroinflammation and oxidative stress (OS) [5]. Therefore, how to effectively inhibit inflammation and reduce EBI has become an important therapeutic target for aSAH.

Many naturally derived bioactive compounds have become the focus in recent years. Eriocitrin (EC), primarily extracted from citrate orange or lemon juice, is a kind of flavonoid with a protective effect on human health [6]. EC exhibits various pharmacological actions, including but not limited to anti-diabetic, anticancer, antioxidation, and anti-steatosis activities [7]. EC has been reported to reduce liver oxidative damage in rats [8]. Hence, it has become a research hot spot to investigate the bioactivity of EC as well

as its mechanisms and pharmacokinetics in diseases. However, systematic conclusions or evidence on the efficacy of EC against inflammation and OS in SAH are difficult to track in literature.

Similarly, the role and mechanism of EC in injury diseases have not been thoroughly studied. EC has been indicated to play a role primarily by suppressing nuclear factor-κB (NF-κB) [9], but the associated mechanism has not been explored in depth. Studies have reported that EC can exert antioxidant effects and inhibit inflammation by upregulating dual specificity phosphatase 14 (DUSP14) [10]. DUSP14, or MKP6, is an atypical DUSP, as it has a consistent DUSP C-terminal catalytic domain but no N-terminal CH2 domain [10]. By dephosphorylating and inactivating mitogen-activated protein kinases (MAPKs), including signaling molecules such as c-Jun N-terminal kinases (JNKs), p38, and extracellular signal-regulated kinases 1/2 (ERK1/2), DUSP14 modulates cellular responses such as differentiation, OS, proliferation, and immunologic defense [11,12]. SAH damage can eventually activate NF-κB, aggravating inflammatory reactions and OS [13]. Therefore, we speculate that DUSP14 can significantly reduce NF-κB activation in SAH.

DUSP14 may also have antioxidant activity and protective action in multiple injury diseases [14]. At the same time, DUSP14 overexpression can significantly reduce reactive oxygen species (ROS) production and downregulate interleukin (IL)-1β and tumor necrosis factor (TNF)-α by regulating the protein kinase TGF-β activated kinase 1 (TAK1) signaling pathway, thus protecting mice from brain ischemia/reperfusion (I/R) damage [15]. OS and inflammatory response factors (TNF-α, IL-1β, etc.) greatly interfere with the occurrence and development of SAH. Therefore, the regulatory role of DUSP14 may be critical in SAH.

Accordingly, the present research aims to investigate the anti-OS and remedial inflammatory response of EC in SAH-induced EBI in an experimental animal and cell model.

Data and Methods

SAH Model and Groups

80 Male Sprague Dawley (SD) rats (weight 220–250 g), ordered from the Animal Experiment Center, Wuhan University, were caged and fed routinely under the environment of 20~25 °C (temperature), 50%~52% (humidity) and a 12 hour light/dark cycle. According to reference [16], the SAH model was established by internal carotid artery (ICA) puncture. The details are as follows. After intraperitoneal anesthesia using 10 g/L pentobarbital sodium (35 mg/kg), 80 rats were fastened in a supine position to expose the common, ICA and external carotid arteries (ECA), with the ECA ligated, through which a 4-0 nylon wire was inserted into the ICA until resistance was felt, and a further 5-mm insertion was performed to penetrate the ICA wall. The sham operation group (randomly choose 15 rats) received the same operation except that the ICA was not punctured. This experimental animal ethics were passed without reservation by the ethics committee of Renmin Hospital of Wuhan University (ethics code: #20210653), and all procedures were conducted strictly following the national institutes of health guidelines for the feeding, management and use of experimental animals.

63 rats were successfully modeled (sham group excluded), and the success rate of modeling was 96.9%. The SAH rats were randomly assigned to SAH, SAH+Saline and SAH+EC (25 mg/kg, RiboBio, Guangzhou, China), and SAH+Eriodocitrin (EC)+ protein-tyrosine-phosphatase (PTP) inhibitor IV (specific DUSP14 inhibitor, 50 µM/mL, San Diego, CA, USA) groups, with 15 rats in each group. And then there's the sham group (15 rats). The rest 3 rats were used as back up rats. Then, ECs (25 mg/kg) [17] were intraperitoneally injected once a day, for 3 days before modeling and throughout the experiment. For the SAH+Eriodocitrin+PTP inhibitor IV group, PTP inhibitor IV was administered once daily at 5 mg/kg via the tail vein 3 days before modeling and throughout the experiment on the basis of Eriodocitrin treatment.

Morris Water Maze Test

We performed Morris Water Maze (MWM) tests to assess rats' spatial learning and memory function. The MWM is a four-quadrant round pool (120 cm, 50 cm, and 31 cm in diameter, height, and water depth, respectively), with a circular platform below the horizontal plane (10 cm in diameter, 30 cm in height, and 1 cm below water depth) that was positioned at the 2nd quadrant 20 cm away from the pool wall and the water temperature maintained at 24.1 °C. The reference materials around the pool remained constant throughout the experiment. The image acquisition system (ANY-maze®; Stoelting, Wood Dale, IL, USA) placed above the MWM synchronously recorded the movement of the experimental rats. 1 Spatial learning ability evaluation: During the 5-day training, each rat completed training 4 times a day. Each time, the animals were lowered into the water from a different quadrant facing the pool wall, and the time it took them to climb onto the platform (latency) was recorded. They were further instructed to step onto the platform and stayed there for 20 s. The latency was recorded as 120 s upon their failure to find the platform within 120 s. After daily training of rats, their mean escape latencies were counted. Spatial memory assessment: After removal of the 2nd quadrant platform 24 hours after the learning ability test, the rats were placed in water facing the wall from the four quadrants. The navigation time looking for the target (2nd) quadrant's platform within 60 seconds was recorded.

Modified Neurological Severity Scores

Five experimental rats were randomly selected from each group for modified neurological severity scores

(mNSS) assessment 24 hours after SAH. According to the mNSS, the researchers who did not know the experimental group and received professional training were blindly scored. mNSS mainly evaluated the following five aspects: walking, sensation, tail lifting, balance and loss of reflex on days 1, 3, 7, 14, and 28, respectively. The score ranges from 0 (completely normal with no neurological impairment) to 18 (loss of consciousness or death). The rats with a mNSS score of 13 to 14 were selected as random replacement candidates in later experiments.

Dry–Wet Method

On the 3rd day after successful modeling (6th day after treatment), 5 rats were randomly selected in each group and the rat brain water content (BWC) was detected by the Dry–Wet (DW) method. Autonomous breathing rats were anesthetized by inhalation of an oxygen-air mixture of 1–2% isoflurane through a mask. After being weighed, they were sacrificed by exsanguination from a cardiotomy performed under deep isoflurane anesthesia. During bloodletting, the head was elevated to ensure blood drainage from the brain. The fresh cerebral cortex was collected from the edge of the bone window and weighed on an electronic analytical balance for its wet mass (WM). After that, dry mass (DM) measurement was performed by wrapping the sample in a tin foil with a known weight and baking it in a 100 °C oven for 24 h. BWC (%) = [(WM-DM)/WM] × 100%.

Immunohistochemistry

Immunohistochemistry (IHC) was utilized for cellular DUSP14 detection. The fixed tissue was subjected to dehydration, embedding and slicing for 1 h of baking at 60 °C. The slices were then successively dewaxed for 5 minutes in xylene I, II, and III, followed by 5 minutes of immersion in anhydrous, 95%, and 75% ethanol. After tap water rinsing (5 min) as well as microwave retrieval (10 min) in citric acid buffer, the slices were treated with room temperature cooling and 0.3% hydrogen peroxide addition for a 15-minute cultivation in a wet box and the subsequent 30-minute cultivation in a 37 °C wet box. After mixing the slices with an anti-DUSP14 antibody (ab272587, 1:100, Abcam, Cambridge, MA, USA), they were cultivated overnight (4 °C), followed by diaminobenzidine (DAB) staining with a 20-minute incubation in a 37 °C wet box. After rinsing with tap water, it was dehydrated, transparent and sealed. Illumination and imaging were performed using a fluorescence microscope (Leica DMI8, Leica Microsystems Co., LTD, Wetzlar, Germany). The average gray level of the positive expression site was observed and analyzed by Imageproplus software 6.0 (Media Cybernetics, Inc., Bethesda, MD, USA).

Immunofluorescence

Paraffin tissue samples were sliced, conventionally dewaxed into water, and placed in Tris EDTA buffer solution (pH 8.5), followed by 20 minutes of microwave heating for antigen retrieval and 30 minutes of room temperature sealing with 5% donkey serum. After disposal of serum, an anti-Iba-1 antibody (1:100) was dripped for culture at 4 °C overnight. This was followed by phosphate-buffered saline (PBS) washing for 5 minutes × 3 times, fluorescent secondary antibody (1:100) addition, and ambient temperature incubation (1 h). Following PBS washing, we observed and imaged the samples under a fluorescence microscope (Carl Zeiss, Göttingen, Germany) and detected the expression of microglial cells. The Image J (version 1.50, National Institutes of Health, Bethesda, MD, USA) was used to assess the number of microglia, and were determined over 5 separate experiments.

TUNEL Staining

Fourteen days after modeling, the brain tissue of the remaining 5 rat hippocampus was collected for TUNEL staining as per the manuals of the TdT-mediated dUTP Nick-End Labeling (TUNEL) kit (Roche Diagnostic Systems, Branching, NJ, USA). Following 15 minutes of baking at 60 °C, the slices were treated with xylene dewaxing and gradient ethanol dehydration, followed by room temperature treatment with protease K (10 minutes) and immersion in a TUNEL reaction solution for cultivation (1 h) that was maintained at 37 °C. The slices were placed indoors for 10 minutes after treatment with 3% H_2O_2 methanol and then incubated with transforming peroxidase solution at 37 °C for 30 minutes. This was followed by diaminobenzidine (DAB) staining and hematoxylin redyeing. Next, they were subjected to gradient ethanol dehydration, xylene rising, and resin sealing. TUNEL-positive (+) cells were yellowish brown microscopically, and the apoptosis rate was recorded as TUNEL+ cells/total cell count.

Cell Cultivation and Drug Treatment

The BV2 cell line (Cell Center of Chinese Academy of Sciences, Shanghai, China, #1101MOU-PUMC000063) was placed in RPMI1640 (Thermo Fisher Scientific, Waltham, MA, USA) culture medium supplemented with fetal bovine serum (FBS; 10%; Thermo Fisher Scientific, Waltham, MA, USA) and penicillin/streptomycin (1%; Invitrogen, Carlsba, CA, USA), and the culture was carried out in a 37 °C incubator with a 5% volume fraction of CO_2. Trypsin (0.25%), ordered from Thermo Fisher HyClone, Utah, USA, was utilized for logarithmic growth-phase cell digestion and passage. Mycoplasma testing was performed and confirmed that the results were negative for the BV2 cells used in the experiments.

For the *in vitro* SAH model, oxyhemoglobin (OxyHb, Bio Basic Inc., Amherst, NY, USA) was used for culture system stimulation. We grouped microglia as follows: control, OxyHb, OxyHb+EC (1 μM/mL, 2 μM/mL, or 4 μM/mL), and OxyHb+EC+PTP inhibitor IV (specific DUSP14 inhibitor, 50 μM, San Diego, CA, USA). The cul-

Table 1. Primer sequences of the genes.

Gene	Primer sequences (5′ → 3′)
DUSP14	forward:GCTTCGGCAGCACATATACTAAAAT
	reverse:CGCTTCACGAATTTGCGTGTCAT
TNF-α	forward:CAGGGGCCACCACGCTCTTC
	reverse:CTTGGGGCAGGGGCTCTTGA
IL-6	forward:ATGAACTCCTTCTCCACAAGCGC
	reverse:GAAGAGCCCTCAGGCTGGACTG
IL-1β	forward:TCCCTTCATCTTTGAAGAAGA
	reverse:GAGGCCCCAAGGCCACAGG
GAPDH	forward:TGATCTTCATGGTCGACGGT
	reverse:CCACGAGACCACCACCTACAACT

DUSP14, dual specificity phosphatase 14; *TNF*, tumor necrosis factor; *IL*, interleukin; *GAPDH*, glyceraldehyde 3-phosphate dehydrogenase.

ture media and cells were collected for RT–PCR, Enzyme-linked immunosorbent assay (ELISA), Western blot, etc.

Quantitative Real–Time PCR

All procedures in this experiment followed the recommendations of the corresponding kit or instrument. Total RNA was extracted by TRIzol reagent for qRT–PCR. RNA was inversely recorded as cDNA using the PrimeScript recording RT Reagent kit (Invitrogen, Shanghai, China), and qRT–PCR was performed with a Bio-Rad CFX96 quantitative PCR system plus SYBR. qRT–PCR conditions: predenatured (95 °C), denatured (95 °C), and annealed (60 °C) for 5 minutes, 15 s, and 30 s, respectively. In qRT–PCR, DUSP14, TNF-α, IL-6 and IL-1β were normalized against glyceraldehyde 3-phosphate dehydrogenase (GAPDH). All qRT–PCR responses were run in triplicate. Gene expression was calculated using the $2^{-\Delta\Delta Ct}$ method. Guangzhou Ruibo Company was responsible for primer design and synthesis, and the primer sequences are shown in Table 1.

Western Blot

For western blot (WB), collected tissues or cells were treated with three cold PBS rinses and 100~200 µL RIPA lysis buffer (Beyotime Biotechnology, Shanghai, China). Following ultrasonic lysis of cells in ice water, protein concentrations were identified using the Bradford method. From each group, the same amount of protein was used for SDS–PAGE (10%) electrophoresis, followed by protein loading onto a PVDF membrane (Millipore, Bedford, MA, USA) for 1 h of blocking at 4 °C. The following primary antibodies, all ordered from Abcam, Cambridge, UK and diluted at 1:1000, were added overnight at 4 °C: anti-DUSP14 (ab134265), anti-Nrf2 (nuclear factor erythrocyte-2-related factor 2; ab137550), anti-NF-κB (ab32536), anti-pNF-κB (ab86299), anti-iNOS (inducible nitric oxide synthase; ab178945), anti-COX2 (cyclooxygenase-2; ab15191), anti-HO-1 (heme oxygenase-1; ab68477), anti-NOD-like receptors family pyrin domain containing 3 (NLRP3; ab263899), anti-ASC (apoptosis-associated speck-like protein containing a caspase recruitment domain; ab180799), anti-caspase-1 (ab179515), and anti-GAPDH (ab8245). The membrane, after two TBST washes, was then incubated indoors for 1 h with a fluorescein-labeled secondary antibody (ab205718, 1:2500, Abcam, Cambridge, UK). The membrane was finally exposed with the use of an ECL chromogenic agent (Millipore, Bedford, MA, USA) and imaged using a film scanner after three rinses. The relative expression of the protein bands was quantified by densitometric scanning of the X-ray films with GS-700 Imaging Densitometer (GS-700, Bio-Rad Laboratories, Milan, Italy) and a computer program (Molecular Analyst, IBM Corp. Armonk, NY., USA), and standardized for densitometric analysis to β-Actin levels.

Enzyme-Linked Immunosorbent Assay

According to the grouping, the cells were centrifuged at 4 °C and 1000 ×g by Enzyme-linked immunosorbent assay (ELISA), with the supernatant collected to determine IL-1β, IL-6 and TNF-α contents as well as OS-associated indexes (malondialdehyde (MDA), superoxide dismutase (SOD) and glutathione peroxidase (GSH-px)) in rat brain homogenate supernatant or cell supernatant as per the corresponding ELISA kit instructions. The IL-1β, IL-6 and TNF-α kits were from Multisciences (lianke) Biotech (Hangzhou, China): IL-1β (#EK301B), IL-6 (#EK360), TNF-α (#EK382); The MDA, SOD and GSH-px kits were from Nanjing Jiancheng Bioengineering Institute (Nanjing, China): MDA (#A003-1-2), SOD (#A001-1-2) and GSH-px (#A005-1-2).

Statistical Analysis

All results were input into SPSS24.0 (SPSS Inc., Chicago, IL, USA) for data processing and analyses and are denoted by the mean ± standard deviation (SD). The comparison methods included the *t* test for the two groups of data, as well as the one-way ANOVA for multigroup differences and the following Tukey post hoc test for pairwise comparisons. GraphPad8.0 software (GraphPad Software Inc., San Diego, CA, USA) was utilized for graphing, and significant differences were reported at the $p < 0.05$ level.

Results

EC could Reduce SAH-Induced Neuronal Apoptosis and Neurological Impairment

To explore the protective action of EC against SAH-induced neuronal apoptosis and neurological impairment, we established an animal model of SAH and treated with EC (25 mg/kg). The post injury cognitive, learning and motor functions of the experimental rats were verified by mNSS and MWM tests. SAH rats showed increased mNSS scores compared with sham rats (Fig. 1A), with a prolonged

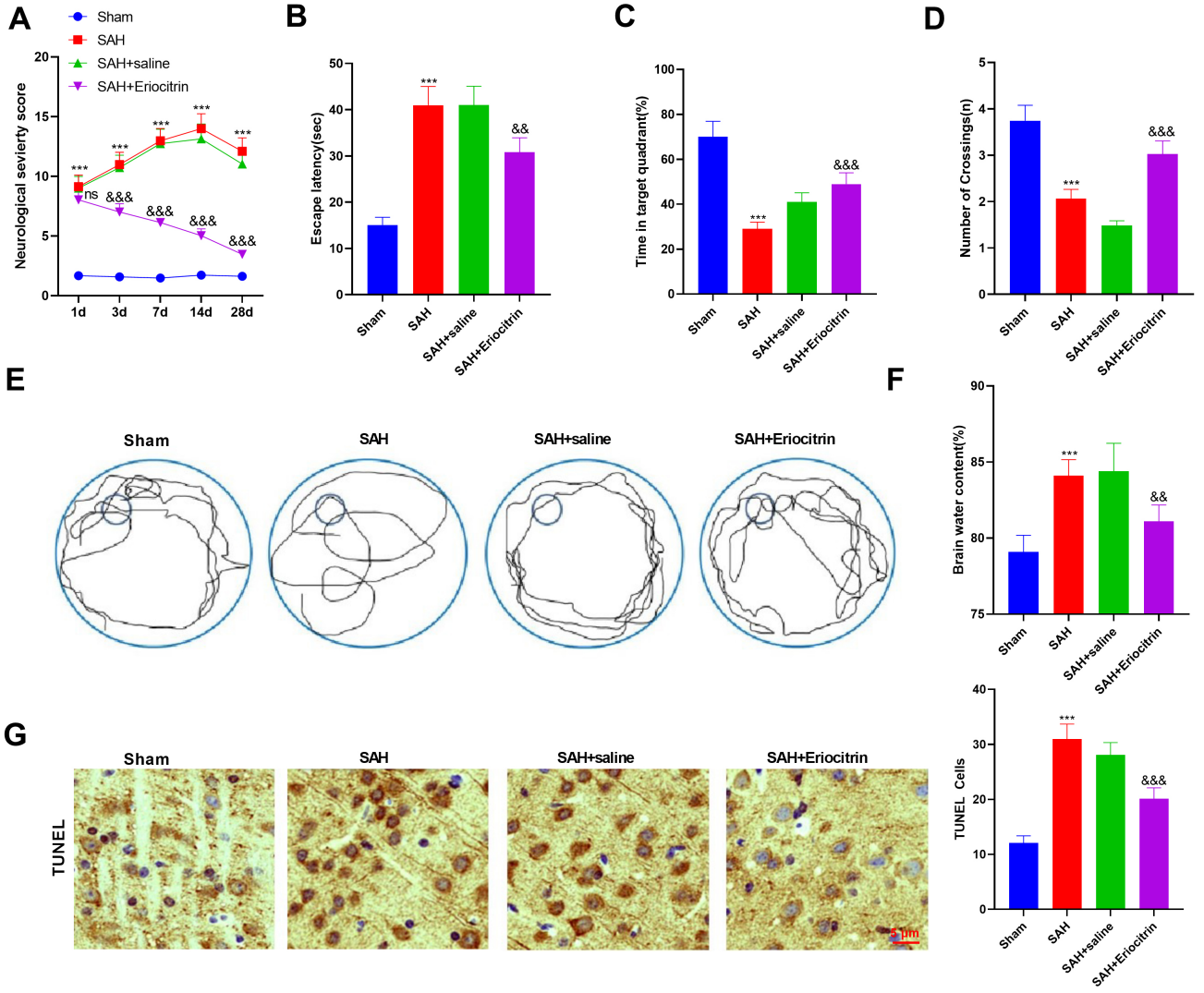

Fig. 1. Eriocitri (EC) could attenuate neuronal apoptosis and neurological damage induced by SAH. (A) mNSS score was used to measure neurological function after SAH. (B–E) The escape latency, target quadrant time and platform crossing times of the Morris water maze test were measured 72 hours after SAH. (F) Brain edema detected on the 3rd day post SAH by the dry–wet method. (G) Rat neuronal apoptosis measured by TUNEL staining. *** indicate $p < 0.001$, respectively (vs. Sham group), ns, && and &&& indicate $p > 0.05$, $p < 0.01$, and $p < 0.001$, respectively (vs. SAH+saline). Data are expressed as the mean ± SD (n = 5). EC, Eriocitrin; SAH, subarachnoid hemorrhage; mNSS, modified neurological severity scores; SD, standard deviation; TUNEL, TdT-mediated dUTP Nick-End Labeling.

latency to search for the underwater platform and decreased residence time and crossing times in the platform quadrant ($p < 0.05$, Fig. 1B–D). EC (25 mg/kg) treatment decreased the mNSS score ($p < 0.05$, Fig. 1A), reduced escape latency, prolonged platform quadrant residence, and increased platform quadrant crossings ($p < 0.05$, Fig. 1B–E). In addition, rat BWC was measured on day 3 after modeling using the DW method. Higher BWC was found in SAH rats versus sham rats, which decreased significantly after EC treatment ($p < 0.05$, Fig. 1F). Finally, TUNEL staining results revealed a notably higher TUNEL+ cell count in the SAH group than in the sham group. However, EC significantly lowered the TUNEL+ cell count ($p < 0.05$, Fig. 1G). This suggests the ability of EC to significantly attenuate central nervous system (CNS) injury and neuronal apoptosis during SAH in rats.

EC Significantly Inhibited the Oxidative Stress and Inflammation in SAH Rats

Inflammation and OS triggered by SAH are the most important mechanisms of secondary injury in the CNS. First, we detected Iba1 expression in SAH rat brain tissues by immunofluorescence. The SAH group exhibited a higher number of Ibal cells than the Sham group, which was markedly suppressed by EC ($p < 0.05$, Fig. 2A). In addition, SAH rats showed markedly elevated IL-1β, TNF-α,

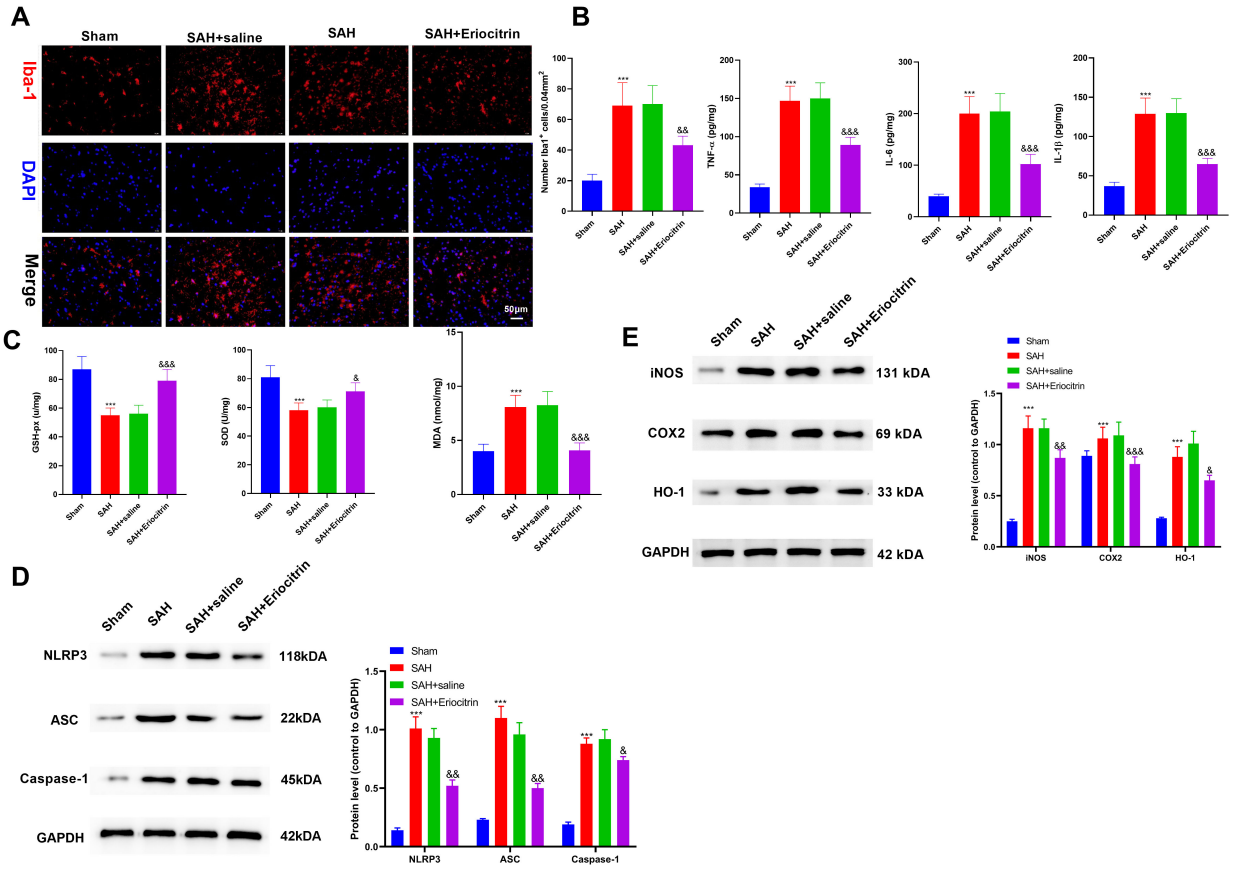

Fig. 2. EC significantly inhibited oxidative stress and inflammation in the brain tissue of SAH rats. (A) The activation of microglia was detected by immunofluorescence (Iba-1 labeling in red, nucleus labeling in blue). (B,C) ELISA measurements of inflammatory factors (IL-1β, IL-6, TNF-α) and oxidative stress (MDA, SOD and GSH-px) in SAH rat brain tissue (hippocampus). (D) Western blotting of NLRP3/ASC/Caspase-1 in rat brain tissue. (E) Western blotting of iNOS, COX2 and HO-1 protein levels in rat brain tissue. *** indicate $p < 0.001$ (vs. Sham group), &, &&, and &&& indicate $p < 0.05$, $p < 0.01$, $p < 0.001$, respectively (vs. SAH+saline). Data are expressed as the mean $\pm$ SD (n = 5). ELISA, Enzyme-linked immunosorbent assay; iNOS, inducible nitric oxide synthase; COX2, cyclooxygenase-2; HO-1, heme oxygenase-1; NLRP3, NOD-like receptors family pyrin domain containing 3; ASC, apoptosis-associated speck-like protein containing a caspase recruitment domain; MDA, malondialdehyde; SOD, superoxide dismutase; GSH-px, glutathione peroxidase.

IL-6 and MDA levels and reduced SOD and GSH-px activities compared with sham rats, as indicated by ELISA results. EC lowered the release of inflammatory cytokines and MDA and elevated SOD and GSH-px activities ($p <$ 0.05, Fig. 2B,C). Based on WB, NLRP3/ASC/Caspase-1 protein expression was significantly lower in the EC group than in the SAH group (Fig. 2D). Finally, the SAH group had higher iNOS, COX2 and HO-1 expression than the sham group, which was markedly reduced by EC treatment ($p < 0.05$, Fig. 2E). Therefore, EC attenuated inflammation and OS in SAH rats.

EC Regulated the NF-κB Pathway and Upregulated DUSP14

To identify whether EC attenuates SAH-induced CNS damage by upregulating the expression of DUSP14 to regulate NF-κB pathways, DUSP14 measurements were made by RT–PCR, WB and IHC. Brain tissue DUSP14 was found to be significantly inhibited after SAH, while EC could promote DUSP14 expression ($p < 0.05$, Fig. 3A–C). Additionally, EC elevated Nrf2 expression and inhibited NF-κB activation ($p < 0.05$, Fig. 3C). This results suggested that EC upregulated Nrf2 and DUSP14 while significantly inhibiting NF-κB activation.

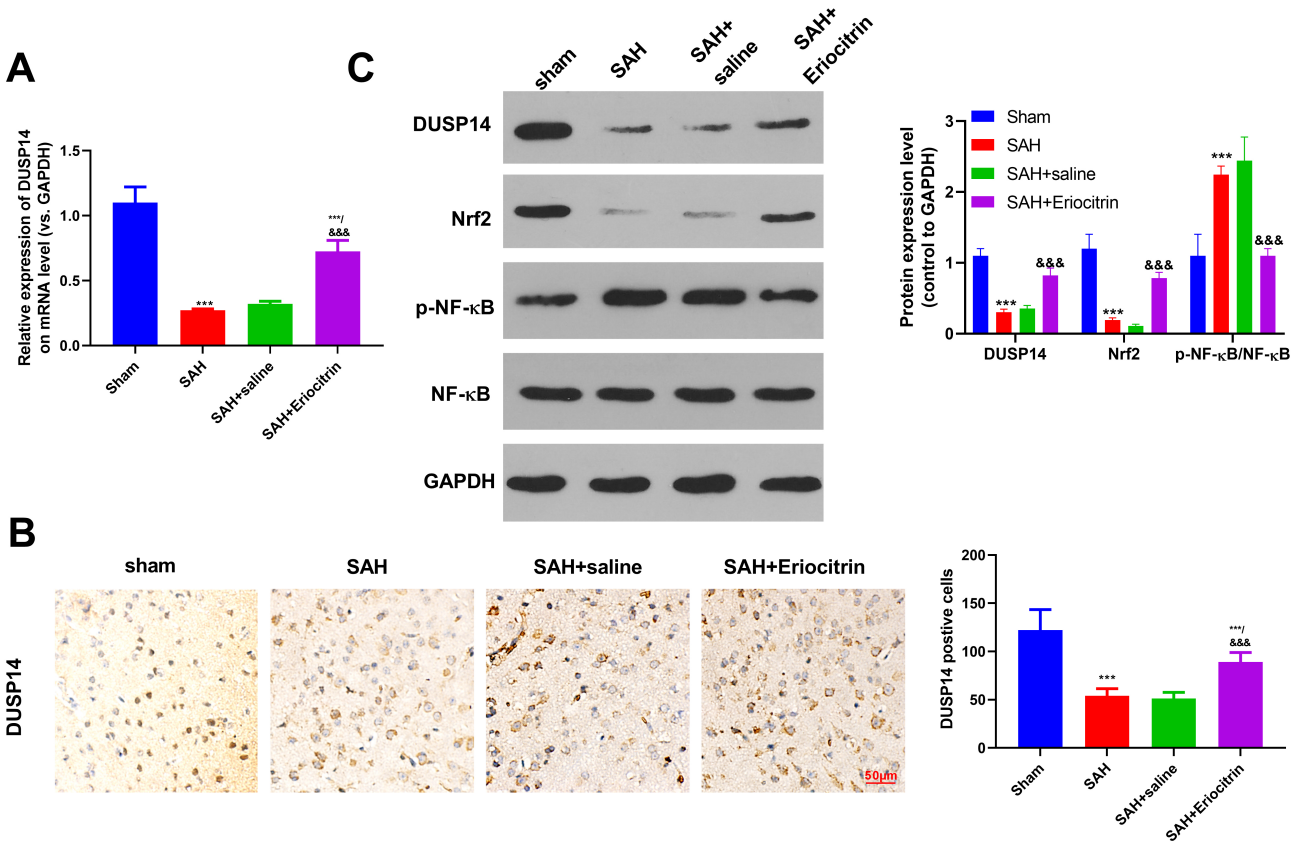

Fig. 3. EC regulated the NF-κB axis and increased DUSP14 expression. (A) RT–PCR quantification of DUSP14 mRNA changes. (B) IHC detection of DUSP14 expression in the SAH rat cortex. (C) WB quantification of brain tissue DUSP14, Nrf2 and NF-κB expression after SAH. *** indicate $p < 0.001$ (vs. Sham group), &&& indicate $p < 0.001$, respectively (vs. SAH+saline). Data are expressed as the mean $\pm$ SD (n = 5). NF-κB, nuclear factor-κB; IHC, Immunohistochemistry; WB, Western Blot; Nrf2, nuclear factor erythroid-2-related factor 2.

DUSP14 Suppression could Reverse EC's Protection

Furthermore, we used a DUSP14-specific inhibitor, PTP inhibitor IV, to inhibit DUSP14 to determine whether suppressing DUSP14 reversed EC protection against SAH. Also, as shown in Figs. 1, 4, according to mNSS and Morris water maze test results, this inhibitor reversed the protective action of EC, decreased the cognitive function of rats, increased the mNSS score, prolonged the escape latency, and decreased the platform quadrant residence and the number of platform crossings ($p < 0.05$, Fig. 4A–C). In addition, IFs (IL-1β, TNF-α and IL-6) increased significantly as the PTP inhibitor IV was added compared with the EC only, as indicated by ELISA ($p < 0.05$, Fig. 4D). PTP inhibitor IV also reversed EC's inhibitory effects on MDA, while notably lowering SOD and GSH-px contents ($p < 0.05$, Fig. 4E). DUSP14, Nrf2 and NF-κB alterations were further identified using WB and IHC, which revealed markedly reduced DUSP14 and Nrf2 levels and enhanced NF-κB activation by PTP inhibitor IV ($p < 0.05$, Fig. 4F,G). Thus, PTP inhibitor IV could reverse EC protection by inhibiting DUSP14, thus aggravating SAH-mediated CNS injury.

EC Significantly Inhibited OxyHb-Induced Inflammation and OS in Vitro

To further investigate the regulatory action of EC against inflammation and OS in microglia, BV2 cells were subjected to OxyHb pretreatment for 24 h. As indicated by RT–PCR and ELISA, OxyHb notably increased IFs (IL-1β, IL-6, TNF-α), while EC inhibited these factors in a concentration-dependent manner ($p < 0.05$, Fig. 5A,B). ELISA determined OS responses in each group, and EC was found to markedly suppress MDA induced by OxyHb and increase SOD and GSH-px ($p < 0.05$, Fig. 5C). The above suggests the ability of EC to significantly inhibit inflammation and OS in BV2 cells.

EC Regulated the DUSP14, Nrf2 and NF-κB Pathway

This section explores whether EC alleviates OxyHb-induced BV2 cell injury by upregulating DUSP14, and modulating Nrf2 and NF-κB *in vitro*. RT–PCR and WB quantification of DUSP14 revealed noticeably downregulated DUSP14 in OxyHb-induced BV2 cells, while EC enhanced DUSP14 expression ($p < 0.05$, Fig. 6A,B). EC also

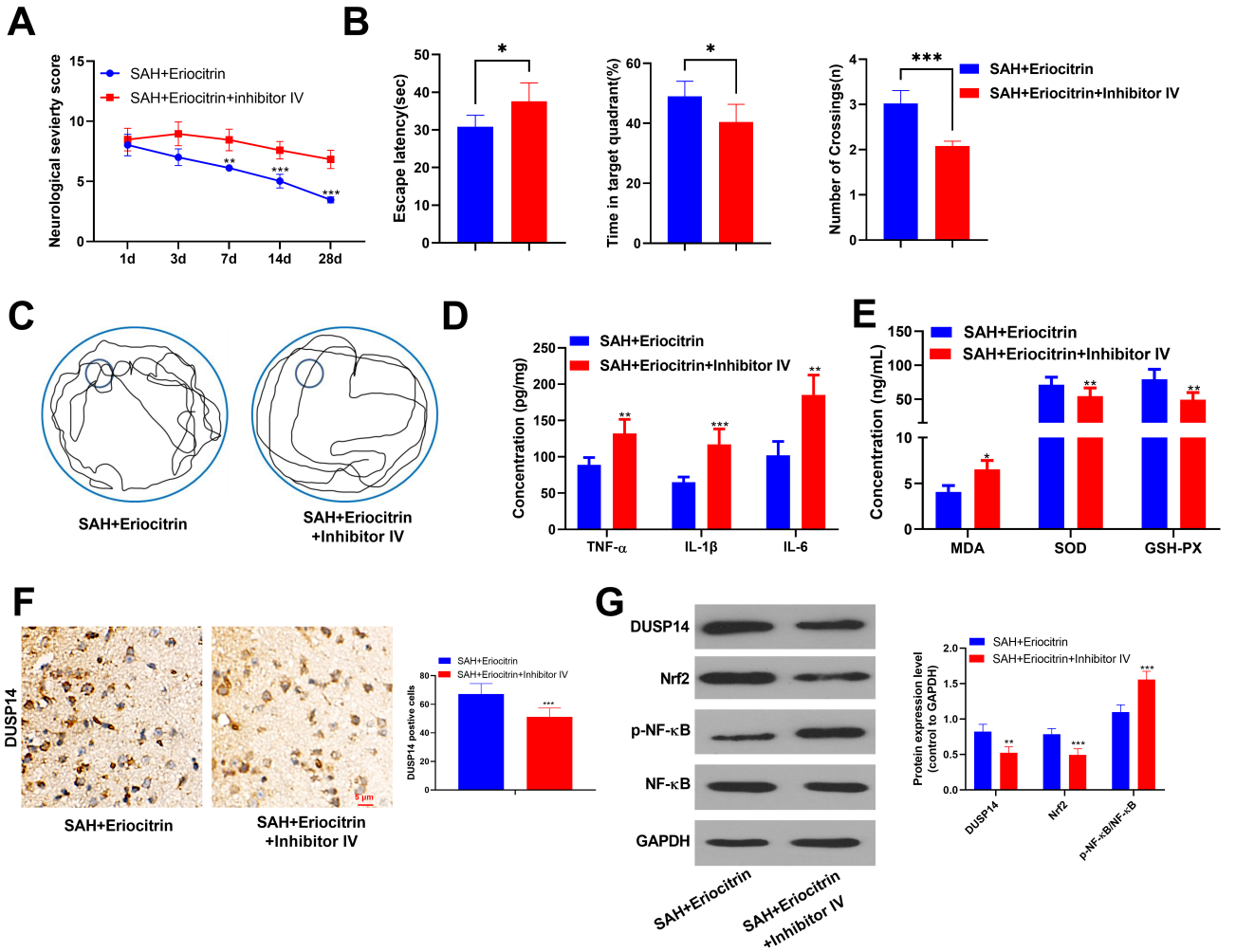

Fig. 4. DUSP14 suppression could reverse EC's protection. (A) mNSS score was used to measure the neurological function score. (B,C) The escape latency, target quadrant time and platform crossing times of the Morris water maze test were measured 72 hours after SAH. (D,E) ELISA measurements of inflammatory factors and oxidative stress (IL-1β, IL-6, TNF-α, MDA, SOD and GSH-px) in SAH rat brain tissue. (F) IHC measurements of DUSP14 in the SAH rat cortex. (G) Western blotting measurements of DUSP14, Nrf2 and NF-κB protein levels in SAH rat brain tissue. *, **, and *** indicate $p < 0.05$, $p < 0.01$, and $p < 0.001$, respectively. Data are expressed as the mean $\pm$ SD (n = 5).

promoted Nrf2 and inhibited NF-κB activation ($p < 0.05$, Fig. 6B). Therefore, EC could up-regulate DUSP14, enhance Nrf2 and obviously suppress NF-κB activation.

DUSP14 Suppression Reversed the Protective Action of EC in Vitro

Furthermore, we used PTP inhibitor IV to suppress DUSP14 to clarify whether DUSP14 suppression could reverse EC's protective action *in vitro*. Based on RT–PCR and ELISA analyses, the PTP inhibitor IV group had notably higher IF (IL-1β, IL-6, TNF-α) levels than the OxyHb + EC (4 µM/mL) group. In addition, the inhibitor reversed EC's impact on MDA, while notably decreasing SOD and GSH-px contents ($p < 0.05$, Fig. 7A–C). Nrf2 and NF-κB changes were determined by WB, which identified markedly downregulated DUSP14 and Nrf2 and enhanced NF-κB activation by PTP inhibitor IV ($p < 0.05$, Fig. 7D). Hence, PTP inhibitor IV could reverse the protective action of EC by inhibiting DUSP14, to aggravate BV2 cell injury in the OxyHb model.

Discussion

The role of traditional Chinese medicine (TCM) extracts in SAH has been well explored. Although surgery is the main treatment for aSAH, calcium antagonist-based drugs play an absolutely dominant role in the treatment of CVS. Acanthopanax senticosus, Salvia miltiorrhiza, Ginkgo, Radix Puerariae, Ligusticum chuanxiong, calculus bovis, persimmon, gynostemma pentaphyllum and other TCMs have been proven to exert positive effects on preventing and treating CVS, among which Salvia miltiorrhiza

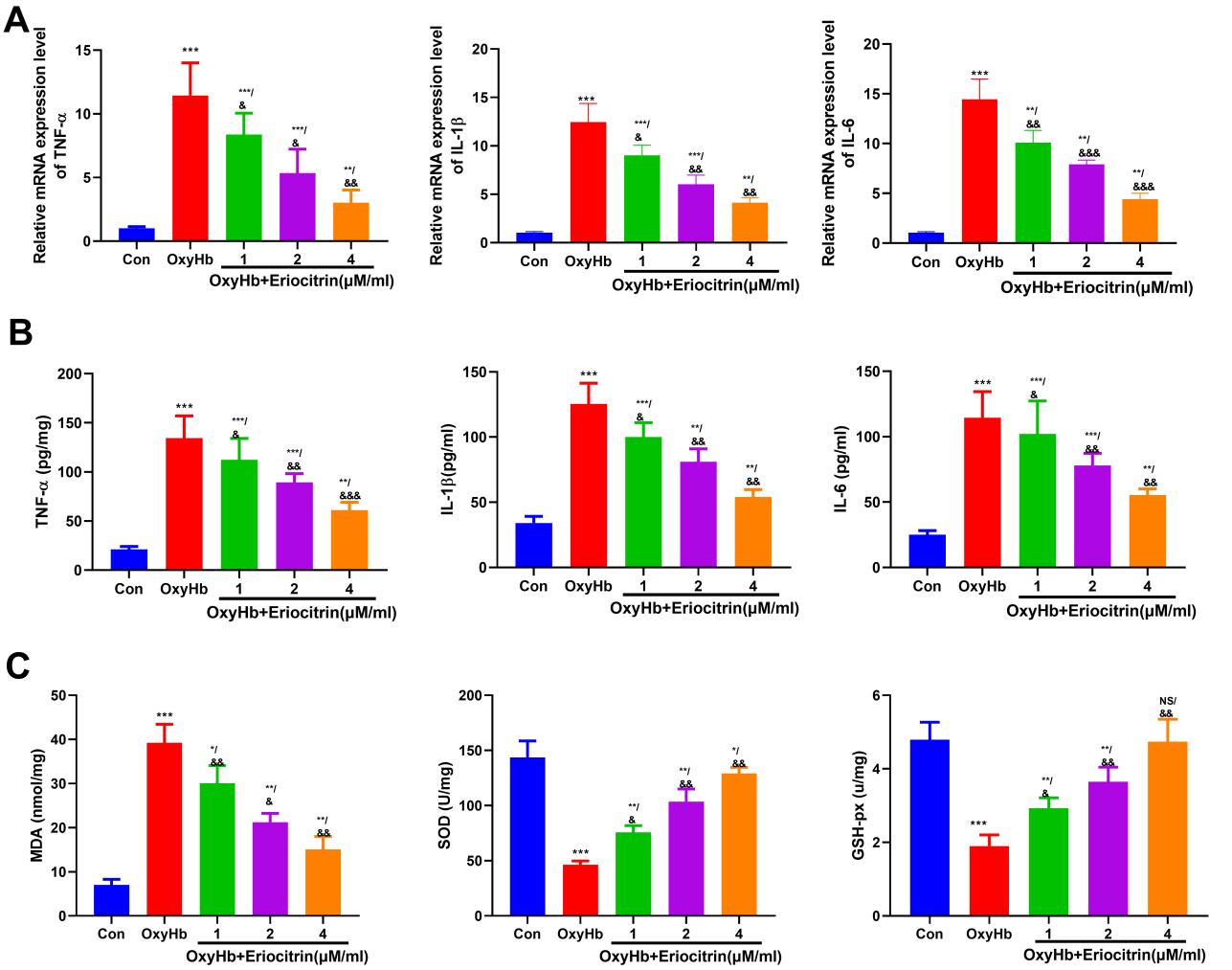

Fig. 5. EC significantly inhibited oxyhemoglobin (OxyHb)-induced inflammation and oxidative stress in BV2 cells. (A) RT–PCR detection of inflammatory factors (IFs; IL-1β, IL-6, TNF-α). (B,C) ELISA measurement of IFs (IL-1β, IL-6, TNF-α) and oxidative stress (MDA, SOD and GSH-px) in the culture supernatant. *, **, and *** indicate $p < 0.05$, $p < 0.01$, and $p < 0.001$, respectively (vs. Con group), NS, &, && and &&& indicate $p > 0.05$, $p < 0.05$, $p < 0.01$ and $p < 0.001$, respectively (vs. OxyHb group). Data are expressed as the mean $\pm$ SD (n = 5).

has a unique influence on bleeding absorption. In addition, aescin and some TCM soups can relieve severe headaches post SAH [18]. Generally, TCM shows unique advantages in SAH treatment, but how to effectively improve the prognosis of SAH patients still requires attention.

Recently, Chinese herbal extracts have been validated to alleviate SAH-induced EBI. Wang F *et al*. [19], for instance, reported that β-caryophyllene liposome (BCP-LP) treatment can significantly alleviate neurological dysfunction and cerebral blood flow perfusion, enhance balance ability in SAH rats. In cerebral edema and blood–brain barrier (BBB) permeability tests, BCP-LP exhibited the ability to reduce post-SAH cerebral edema and accelerate BBB repair. BCP-LP can also reduce the loss of Occludin and Zonula occludens-1, two tight junction proteins, while inhibiting VEGFR-2 and GFAP upregulation and facilitating laminin repair. All the preceding results demonstrate the protective action of BCP-LP against post-SAH NVU (neurovascular unit) in rats [19]. As reported by Peng Y *et al*. [20], magnesium lithospermate B (MLB), a Salvia miltiorrhiza-derived bioactive component, has neuroprotective effects on CNS injury induced by SAH. Intraperitoneal injection of MLB 30 minutes after SAH significantly reduced post-SAH cerebral edema and neurological impairment. Moreover, MLB dose-dependently suppressed microglial activation and neuronal apoptosis and decreased TNF-α and cleaved caspase-3 [20]. Alantolactone (ATL) can alleviate injury to neurons and the cerebral cortex in SAH rats, reduce neurological impairment, inhibit neuronal apoptosis and inflammation, facilitate microglial polarization toward the M2 phenotype, and activate the PI3K/Akt signaling pathway [21]. In addition, the protective effect of other Chinese herbal extracts in SAH has also been reported [22]. These reports confirmed the protective effect

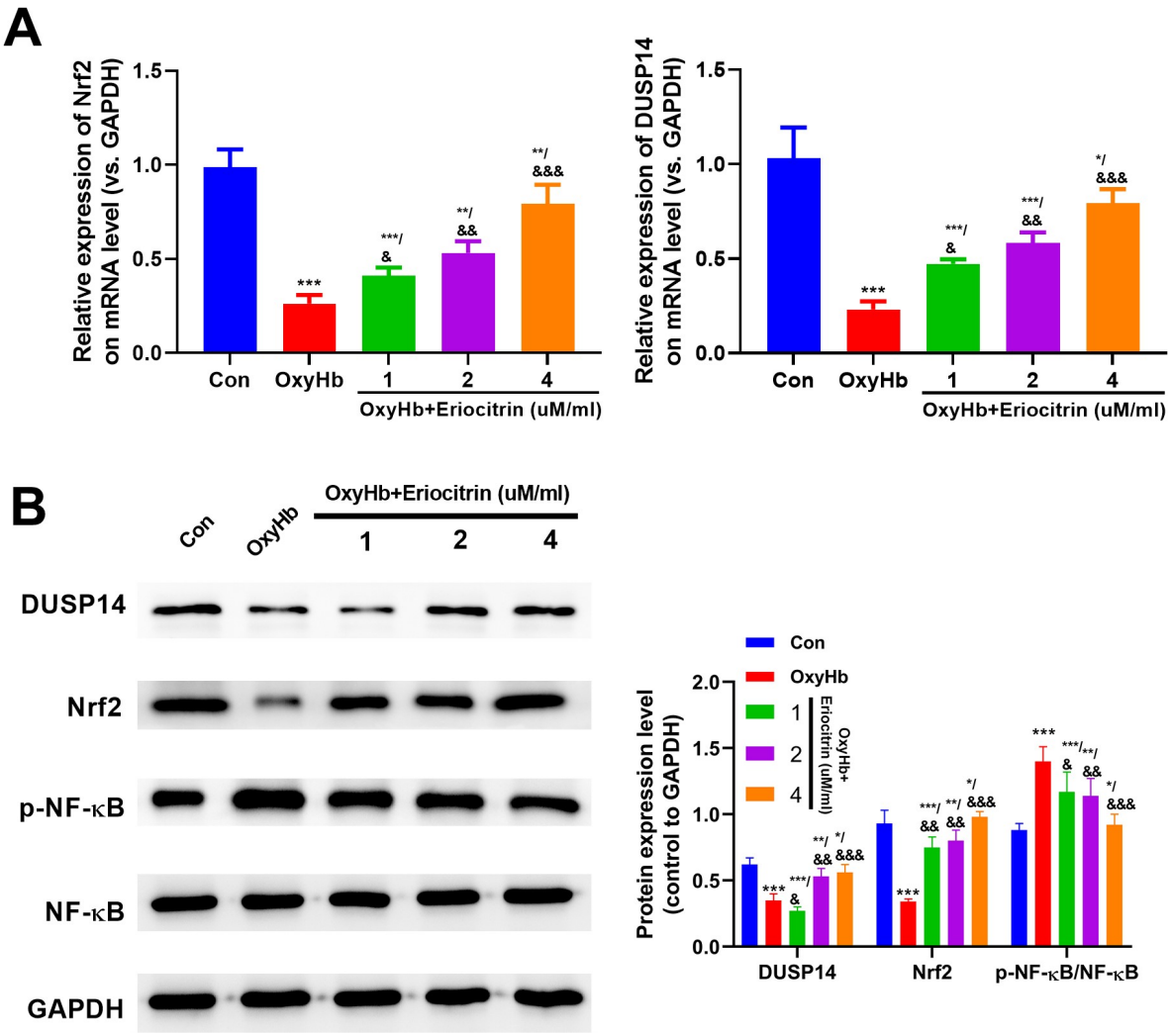

Fig. 6. EC regulated the DUSP14, Nrf2 and NF-κB pathway. (A) RT–PCR measurement of DUSP14 and Nrf2. (B) Western blotting measurement of DUSP14, Nrf2 and NF-κB protein levels in BV2 cells. *, **, and *** indicate $p < 0.05$, $p < 0.01$, and $p < 0.001$, respectively (vs. Con group), &, && and &&& indicate $p < 0.05$, $p < 0.01$, and $p < 0.01$, respectively (vs. OxyHb group). Data are expressed as the mean $\pm$ SD (n = 5). OxyHb, oxyhemoglobi.

of TCM extract in SAH and provided a valuable TCM concept and corresponding theoretical basis for the treatment of SAH. Therefore, this study also focuses on the therapeutic value of a TCM extract in SAH. Our findings showed that EC could play a protective role in reducing SAH-attributed neuronal apoptosis and neurological impairment and inhibit inflammation and OS in SAH.

EC is also known as eriodictyol7-O-beta-rutinoside, and its chemical formula is $C_{27}H_{33}O_{16}$. Studies have shown that EC, a citrus flavonoid, has a high ability to reduce metabolic disorders and obesity-related OS. In a study, randomly dividing 50 male C57BL/6J mice into 5 groups, low-dose EC supplementation was found to reduce serum glucose, blood and liver triacylglycerol in HFD-induced obese mice, demonstrating the ability of EC to mitigate inflammation in all obese mice and its positive effects on OS, systemic inflammation and lipid and glucose metabolism [17]. Recently, the role played by EC in antioxidation has been widely reported. For example, EC has been shown to alleviate diet-induced hepatic steatosis through the activation of mitochondrial transcription factors, nuclear respiratory factors, cytochrome c oxidase subunits, ATP synthases, etc. [23]. Xu J *et al.* [24] found that EC attenuated BUN, serum creatinine and apoptosis induced by I/R in a concentration-dependent manner. At the same time, EC enhanced Nrf-2 levels while blocking NF-κB activation by upregulating DUSP14, thus attenuating OS and inflammation in rats and playing a role in protecting renal function [24]. EC can also significantly reduce cerebral infarct volume, BWC and brain index. Furthermore, EC treatment can relieve pathological damage, promote cell growth and inhibit apoptosis. Active oxygen species and available an-

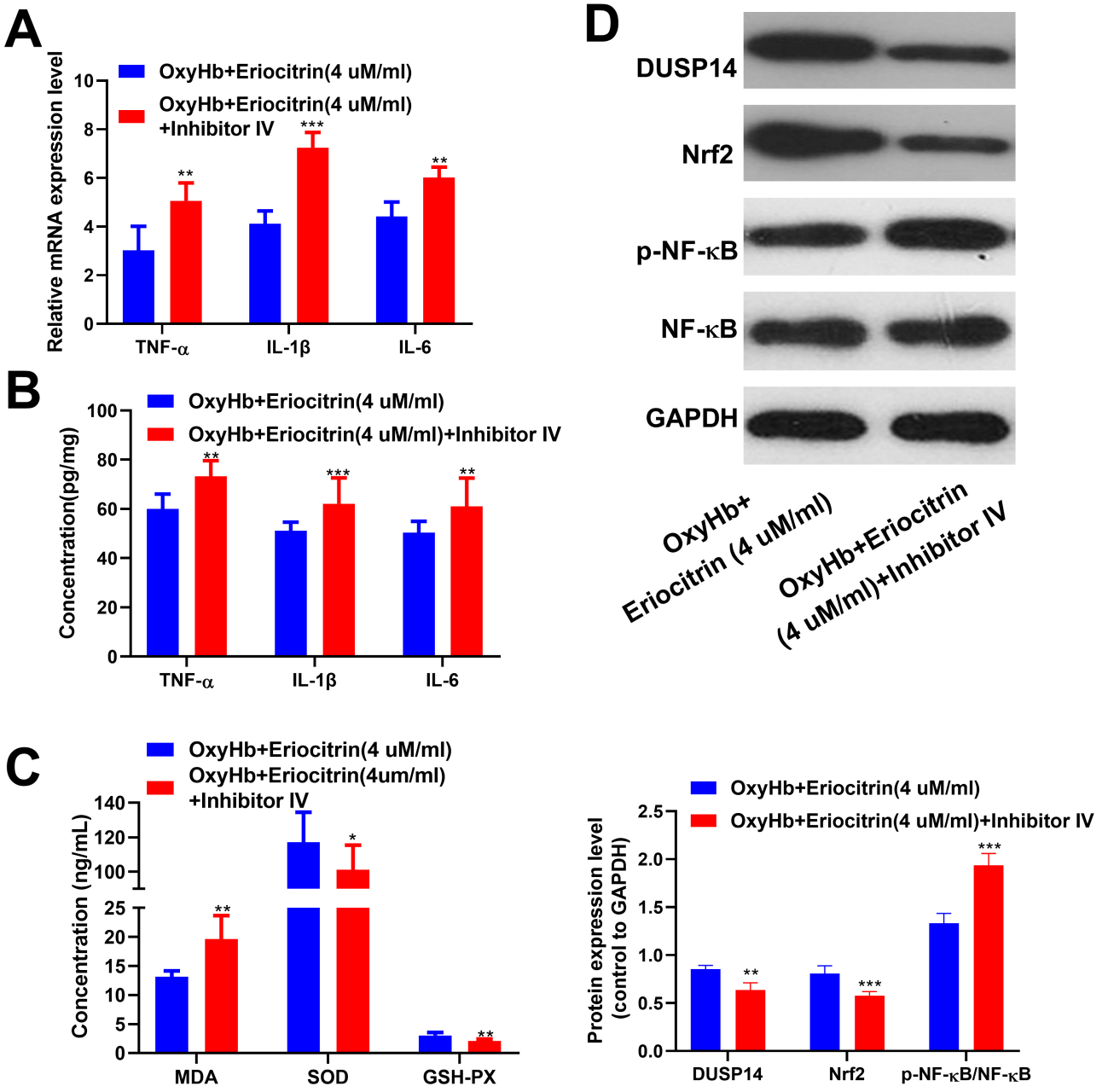

Fig. 7. Inhibition of DUSP14 reversed the protective effect of eriodocitrin on BV2 cells. (A) RT–PCR measurement of cellular inflammatory factors (IFs; IL-1β, IL-6, TNF-α). (B,C) ELISA measurement of IFs (IL-1β, IL-6, TNF-α) and oxidative stress (MDA, SOD and GSH-px) in the culture supernatant. (D) Western blotting measurement of DUSP14, Nrf2 and NF-κB protein levels in BV2 cells. *, **, and *** indicate $p < 0.05$, $p < 0.01$, and $p < 0.001$, respectively. Data are expressed as the mean $\pm$ SD (n = 5).

tioxidant buffering efficiency are on a balance in physiological conditions. Increased levels of the oxidant compound excess the capacity of the antioxidant systems [25]. EC increases SOD activity and decreases MDA and LDH contents. Moreover, it decreased serum and brain tissue IL-6 and TNF-α contents and increased IL-10 levels. In addition, enhanced Nrf2 phosphorylation, reduced NF-κB p65 phosphorylation, and elevated quinine oxidoreductase-1 (NQO1) and HO-1 levels were also observed after EC intervention. A study confirmed that EC attenuates OS damage and inflammation in cerebral ischemia reperfusion (I/R) rats through the Nrf2/HO-1/NQO1/NF-κB axis [26]. Shen Chun-Yan *et al.* [9] reported that EC is the major component of crude polyphenols (CAVAP-W), which can inhibit inflammation and OS, as well as the activation of iNOS, COX-2, and IFs (IL-6, IL-1β, and TNF-α) in LPS-induced RAW264.7 cells. All the above results validate the anti-OS and anti-inflammatory actions of EC. At present, the metabolic process of EC has been reported, which confirmed the distribution of EC *in vivo*, providing a further ba-

sis for the use of EC in clinical practice [27]. Our results are consistent with previous reports, as both animal and cell experiments confirmed that EC could significantly inhibit inflammation in SAH, inhibit the oxidation factor MDA, and increase anti-peroxidation factors SOD and GSH-px levels, playing a significant protective role in SAH.

To further explore the specific mechanism by which EC plays a role, we studied DUSP14, Nrf-2, and NF-κB changes. SAH has been recognized to directly activate JNK and P38 and finally achieve NF-κB activation, thus initiating inflammation and OS responses [28]. Inhibition of NF-κB can significantly reduce injury and improve prognosis, which has been the consensus in the treatment of SAH [29]. As an atypical DUSP, DUSP14 belongs to the DUSP family, with multiple studies reporting its antioxidant and anti-inflammatory actions in injuries and repair [30,31]. DUSP14 overexpression protected mice from brain I/R damage by upregulating the Nrf-2 axis to significantly reduce ROS production and downregulate TNF-α and IL-1β [32]. This report is also the only report of DUSP14 in CNS damage and repair. Thus, the change and value of DUSP14 in SAH still need to be discussed in depth. Our study is consistent with Jianrong Song's [32] report that DUSP14 is significantly decreased in SAH, and this decrease can be improved by EC treatment.

In other diseases, the role of DUSP14 has also been widely reported. Lin Bin *et al*. [33] reported that knockout of DUSP14 increased myocardial injury in I/R, promoted NF-κB and MAPK axis activation, and increased ROS release. Hong L *et al*. [34] found that activation of DUSP14 can reduce the inflammatory response and apoptosis in bone marrow-derived cells (BMMs) by inhibiting the NF-κB and caspase-3 signaling pathways. Overexpressing DUSP14 also significantly enhanced AMP-activated protein kinase (AMPK)-α activation, and blocking AMPK α significantly eliminated the impact of DUSP14 on the prevention of osteoclast differentiation and the modulation of inflammation and apoptosis [34]. The above reports confirmed that DUSP14 can inhibit the NF-κB pathway and play a protective role in diseases. Our report confirmed the role of DUSP14 in SAH for the first time and found that DUSP14 was significantly downregulated in SAH, while upregulating DUSP14 blocked NF-κB activation, thus playing a protective role.

Conclusion

Conclusively, our study confirms that in SAH, EC inhibits NF-κB activation, attenuates OS and inflammation, and plays a protective role in the CNS by upregulating DUSP14, suggesting the promising therapeutic applications of EC for SAH treatment.

Availability of Data and Materials

The data sets used and analyzed during the current study are available from the corresponding author on reasonable request.

Author Contributions

ML and LS designed the research study, conceived and designed the experiments. ML and LS performed the research. LS, XY, JY, JL, YC and ZW provided help and advice on the experiments. LS, XY, JY and ZW analyzed the data. All authors contributed to editorial changes in the manuscript. All authors read and approved the final manuscript. All authors have participated sufficiently in the work and agreed to be accountable for all aspects of the work.

Ethics Approval and Consent to Participate

This experimental animal ethics were passed without reservation by the ethics committee of Renmin Hospital of Wuhan University (ethics code: #20210653), and all procedures were conducted strictly following the national institutes of health guidelines for the feeding, management and use of experimental animals.

Acknowledgment

Not applicable.

Funding

This research received no external funding.

Conflict of Interest

The authors declare no conflict of interest.

References

[1] Petridis AK, Kamp MA, Cornelius JF, Beez T, Beseoglu K, Turowski B, *et al*. Aneurysmal Subarachnoid Hemorrhage. Deutsches Arzteblatt International. 2017; 114: 226–236.

[2] Neifert SN, Chapman EK, Martini ML, Shuman WH, Schupper AJ, Oermann EK, *et al*. Aneurysmal Subarachnoid Hemorrhage: the Last Decade. Translational Stroke Research. 2021; 12: 428–446.

[3] Luo X. CXCR2 antagonism attenuates neuroinflammation after subarachnoid hemorrhage. Journal of Stroke and Cerebrovascular Diseases. 2023; 32: 107266.

[4] Chen S, Wu H, Tang J, Zhang J, Zhang JH. Neurovascular events after subarachnoid hemorrhage: focusing on subcellular organelles. Acta Neurochirurgica. Supplement. 2015; 120: 39–46.

[5] Rass V, Helbok R. Early Brain Injury After Poor-Grade Subarachnoid Hemorrhage. Current Neurology and Neuroscience Reports. 2019; 19: 78.

[6] Cesar T, Salgaço MK, Mesa V, Sartoratto A, Sivieri K. Exploring the Association between Citrus Nutraceutical Eriocitrin and

Metformin for Improving Pre-Diabetes in a Dynamic Microbiome Model. Pharmaceuticals (Basel, Switzerland). 2023; 16: 650.

[7] Guo G, Shi W, Shi F, Gong W, Li F, Zhou G, *et al*. Anti-inflammatory effects of eriocitrin against the dextran sulfate sodium-induced experimental colitis in murine model. Journal of Biochemical and Molecular Toxicology. 2019; 33: e22400.

[8] Koopman I, van Dijk BJ, Zuithoff NPA, Sluijs JA, van der Kamp MJ, Baldew ZAV, *et al*. Glial cell response and microthrombosis in aneurysmal subarachnoid hemorrhage patients: An autopsy study. Journal of Neuropathology and Experimental Neurology. 2023; 82: 798–805.

[9] Shen CY, Jiang JG, Huang CL, Zhu W, Zheng CY. Polyphenols from Blossoms of Citrus aurantium L. var. amara Engl. Show Significant Anti-Complement and Anti-Inflammatory Effects. Journal of Agricultural and Food Chemistry. 2017; 65: 9061–9068.

[10] Chuang HC, Tan TH. MAP4K Family Kinases and DUSP Family Phosphatases in T-Cell Signaling and Systemic Lupus Erythematosus. Cells. 2019; 8: 1433.

[11] Chen HF, Chuang HC, Tan TH. Regulation of Dual-Specificity Phosphatase (DUSP) Ubiquitination and Protein Stability. International Journal of Molecular Sciences. 2019; 20: 2668.

[12] Sun F, Yue TT, Yang CL, Wang FX, Luo JH, Rong SJ, *et al*. The MAPK dual specific phosphatase (DUSP) proteins: A versatile wrestler in T cell functionality. International Immunopharmacology. 2021; 98: 107906.

[13] Ji C, Chen G. Signaling Pathway in Early Brain Injury after Subarachnoid Hemorrhage: News Update. Acta Neurochirurgica. Supplement. 2016; 121: 123–126.

[14] Kumar V, Ali Shariati M, Mesentier-Louro L, Jinsook Oh A, Russano K, Goldberg JL, *et al*. Dual Specific Phosphatase 14 Deletion Rescues Retinal Ganglion Cells and Optic Nerve Axons after Experimental Anterior Ischemic Optic Neuropathy. Current Eye Research. 2021; 46: 710–718.

[15] Zhang Y, Wan J, Xu Z, Hua T, Sun Q. Exercise ameliorates insulin resistance via regulating TGFβ-activated kinase 1 (TAK1)-mediated insulin signaling in liver of high-fat diet-induced obese rats. Journal of Cellular Physiology. 2019; 234: 7467–7474.

[16] Li Y, Fei L, Wang J, Niu Q. Inhibition of miR-217 Protects Against Myocardial Ischemia-Reperfusion Injury Through Inactivating NF-κB and MAPK Pathways. Cardiovascular Engineering and Technology. 2020; 11: 219–227.

[17] Ferreira PS, Manthey JA, Nery MS, Spolidorio LC, Cesar TB. Low doses of eriocitrin attenuate metabolic impairment of glucose and lipids in ongoing obesogenic diet in mice. Journal of Nutritional Science. 2020; 9: e59.

[18] Guo L, Yang X, Yang B, Tang G, Li C. Prevalence, in-hospital mortality, and factors related to neurogenic pulmonary edema after spontaneous subarachnoid hemorrhage: a systematic review and meta-analysis. Neurosurgical Review. 2023; 46: 169.

[19] Wang F, Teng Z, Liu D, Wang Y, Lou J, Dong Z. β-Caryophyllene Liposomes Attenuate Neurovascular Unit Damage After Subarachnoid Hemorrhage in Rats. Neurochemical Research. 2020; 45: 1758–1768.

[20] Peng Y, He P, Fan L, Xu H, Li J, Chen T, *et al*. Neuroprotective Effects of Magnesium Lithospermate B against Subarachnoid Hemorrhage in Rats. The American Journal of Chinese Medicine. 2018; 46: 1225–1241.

[21] Zhou F, Wang Z, Xiong K, Zhang M, Wang Y, Wang M. Alantolactone reduced neuron injury via activating PI3K/Akt signaling pathway after subarachnoid hemorrhage in rats. PLoS ONE. 2022; 17: e0270410.

[22] Xiao X, Sun S, Li Y, Cen X, Wu S, Lu A, *et al*. Geniposide attenuates early brain injury by inhibiting oxidative stress and neurocyte apoptosis after subarachnoid hemorrhage in rats. Molecular Biology Reports. 2022; 49: 6303–6311.

[23] Gangadhariah M, Pardhi T, Ravilla J, Chandra S, Singh SA. Citrus nutraceutical eriocitrin and its metabolites are partial agonists of peroxisome proliferator-activated receptor gamma (PPARγ): a molecular docking and molecular dynamics study. Journal of Biomolecular Structure & Dynamics. 2022; 1–21.

[24] Xu J, Ma L, Fu P. Eriocitrin attenuates ischemia reperfusion-induced oxidative stress and inflammation in rats with acute kidney injury by regulating the dual-specificity phosphatase 14 (DUSP14)-mediated Nrf2 and nuclear factor-κB (NF-κB) pathways. Annals of Translational Medicine. 2021; 9: 350.

[25] Murat IA, Özge AC. A Systematic Review of the Literature Regarding the Relationship Between Oxidative Stress and Electroconvulsive Therapy. Alpha Psychiatry. 2022; 23: 47–56.

[26] He J, Zhou D, Yan B. Eriocitrin alleviates oxidative stress and inflammatory response in cerebral ischemia reperfusion rats by regulating phosphorylation levels of Nrf2/NQO-1/HO-1/NF-κB p65 proteins. Annals of Translational Medicine. 2020; 8: 757.

[27] Li L, Feng X, Chen Y, Li S, Sun Y, Zhang L. A comprehensive study of eriocitrin metabolism *in vivo* and *in vitro* based on an efficient UHPLC-Q-TOF-MS/MS strategy. RSC Advances. 2019; 9: 24963–24980.

[28] Pawlowska E, Szczepanska J, Wisniewski K, Tokarz P, Jaskólski DJ, Blasiak J. NF-κB-Mediated Inflammation in the Pathogenesis of Intracranial Aneurysm and Subarachnoid Hemorrhage. Does Autophagy Play a Role? International Journal of Molecular Sciences. 2018; 19: 1245.

[29] Wang Q, Luo Q, Zhao YH, Chen X. Toll-like receptor-4 pathway as a possible molecular mechanism for brain injuries after subarachnoid hemorrhage. The International Journal of Neuroscience. 2020; 130: 953–964.

[30] Shi Y, Li K, Xu K, Liu QH. MiR-155-5p accelerates cerebral ischemia-reperfusion injury via targeting DUSP14 by regulating NF-κB and MAPKs signaling pathways. European Review for Medical and Pharmacological Sciences. 2020; 24: 1408–1419.

[31] Zhao Z, Yang J, Zhang L, Zhou Y. Enhancement of DUSP14 (dual specificity phosphatase 14) limits osteoarthritis progression by alleviating chondrocyte injury, inflammation and metabolic homeostasis. Bioengineered. 2021; 12: 7495–7507.

[32] Jianrong S, Yanjun Z, Chen Y, Jianwen X. DUSP14 rescues cerebral ischemia/reperfusion (IR) injury by reducing inflammation and apoptosis via the activation of Nrf-2. Biochemical and Biophysical Research Communications. 2019; 509: 713–721.

[33] Lin B, Xu J, Feng DG, Wang F, Wang JX, Zhao H. DUSP14 knockout accelerates cardiac ischemia reperfusion (IR) injury through activating NF-κB and MAPKs signaling pathways modulated by ROS generation. Biochemical and Biophysical Research Communications. 2018; 501: 24–32.

[34] Hong L, Ai J, Ma D. Activation of Dusp14 protects against osteoclast generation and bone loss by regulating AMPKα-dependent manner. Biochemical and Biophysical Research Communications. 2019; 519: 445–452.